© 2021. Published by The Company of Biologists Ltd | Journal of Experimental Biology (2021) 224, jeb242135. doi:10.1242/jeb.242135

RESEARCH ARTICLE

The effects of triceps surae muscle stimulation on localized Achilles subtendon tissue displacements

Nathan L. Lehr[1], William H. Clark[1], Michael D. Lewek[2] and Jason R. Franz[1,*]

ABSTRACT

The triceps surae muscle–tendon unit is composed of the lateral and medial gastrocnemius (MG) and soleus (SOL) muscles and three in-series elastic 'subtendons' that form the Achilles tendon. Comparative literature and our own *in vivo* evidence suggest that sliding between adjacent subtendons may facilitate independent muscle actuation. We aim to more clearly define the relationship between individual muscle activation and subtendon tissue displacements. Here, during fixed-end contractions, electrical muscle stimulation controlled the magnitude of force transmitted via individual triceps surae muscles while ultrasound imaging recorded resultant subtendon tissue displacements. We hypothesized that MG and SOL stimulation would elicit larger displacements in their associated subtendon. Ten young adults completed four experimental activations at three ankle angles (−20, 0 and 20 deg) with the knee flexed to approximately 20 deg: MG stimulation ($STIM_{MG}$), SOL stimulation ($STIM_{SOL}$), combined stimulation, and volitional contraction. At 20 deg plantarflexion, $STIM_{SOL}$ elicited 49% larger tendon non-uniformity (SOL–MG subtendon tissue displacement) than that of $STIM_{MG}$ (P=0.004). For $STIM_{SOL}$, a one-way *post hoc* ANOVA revealed a significant main effect of ankle angle (P=0.009) on Achilles tendon non-uniformity. However, peak tendon non-uniformity decreased by an average of 61% from plantarflexion to dorsiflexion, likely due to an increase in passive tension. Our results suggest that localized tissue displacements within the Achilles tendon respond in anatomically consistent ways to differential patterns of triceps surae muscle activation, but these relations are highly susceptible to ankle angle. This *in vivo* evidence points to at least some mechanical independence in actuation between the human triceps surae muscle–subtendon units.

KEY WORDS: Ultrasound, Ankle, Biomechanics, Neuromuscular control, Plantarflexor

INTRODUCTION

A significant portion of the mechanical power needed to walk is generated by the triceps surae (Farris and Sawicki, 2012). Individual muscles of the triceps surae [i.e. medial gastrocnemius (MG), lateral gastrocnemius (LG) and soleus (SOL)] transmit their power through the architecturally complex Achilles tendon. The Achilles tendon is composed of three distinct bundles of tendon fascicles (i.e. 'subtendons') originating from each triceps surae muscle that twist as they descend and attach to the calcaneus (Edama et al., 2015; Szaro et al., 2009; van Gils et al., 1996). We (Clark and Franz, 2018; Franz et al., 2015; Franz and Thelen, 2015) and others (Chernak Slane and Thelen, 2014; Maas et al., 2020) have suspected that the presence of distinct subtendons may allow for some level of independent actuation among the individual triceps surae muscles when generating an ankle moment during functional activity. Indeed, many studies have revealed different neuromechanical contributions and contractile behavior between the uniarticular soleus and biarticular gastrocnemius muscles during walking (Francis et al., 2013; Gottschall and Kram, 2003; Lenhart et al., 2014). However, a clear relationship between the activation patterns of individual muscles of the triceps surae and the resultant displacement patterns of individual subtendons of the Achilles tendon has yet to be clearly defined. Establishing the mechanical independence of individual triceps surae muscle–tendon units (MTUs) in healthy young human adults is vital in understanding deleterious changes due to age and/or pathology.

Using *in vivo* ultrasound imaging, researchers have revealed non-uniform displacement patterns (i.e. greater displacement in deep versus superficial subtendon tissue) in the human Achilles tendon during passive ankle rotation, eccentric loading and walking (Arndt et al., 2012; Franz et al., 2015; Slane and Thelen, 2014). Based on the majority of cadaveric studies (Del Buono et al., 2013; Edama et al., 2015; Szaro et al., 2009; van Gils et al., 1996), these findings suggest that SOL subtendon tissue (deep portion of the Achilles tendon) consistently undergoes more displacement than MG subtendon tissue (superficial portion of the Achilles tendon) during functional activity in young adults. Clark and Franz (2018) added that triceps surae muscle dynamics themselves may play a role in precipitating those characteristic non-uniform Achilles subtendon displacement patterns. Specifically, using dual-probe ultrasound imaging, we revealed that differences in the magnitude of shortening between the MG and SOL positively correlated with differences in tissue displacements in their associated subtendons of the Achilles tendon during maximum voluntary isometric contractions. However, complex inter-muscular patterns of volitional activation may confound the interpretation of emergent subtendon tissue displacements. Equal longitudinal force transmission from each of the MG and SOL muscles to their respective subtendons is unlikely, requiring a specific level of unequal muscle activations to occur. Moreover, compared with the MG and LG, the SOL has greater muscle volume and force-generating capacity, presumably yielding a disproportionate influence on Achilles subtendon tissue displacements (Albracht et al., 2008). Thus, there is a clear need to control for muscle activation to improve our understanding of how triceps surae muscles precipitate non-uniform tendon tissue behavior.

Electrical stimulation provides a non-invasive tool to bypass volitional muscle activation and investigate the relationship between

[1]Joint Department of Biomedical Engineering, UNC Chapel Hill & NC State University, Chapel Hill, NC 27599, USA. [2]Division of Physical Therapy, UNC Chapel Hill, Chapel Hill, NC 27599, USA.

*Author for correspondence (jrfranz@email.unc.edu)

W.H.C., 0000-0002-7082-5986; M.D.L., 0000-0002-1917-5594; J.R.F., 0000-0001-9523-9708

Received 16 December 2020; Accepted 22 June 2021

Journal of Experimental Biology (2021) 224, jeb242135. doi:10.1242/jeb.242135

triceps surae force and resultant Achilles subtendon tissue displacement. Using electrical muscle stimulation, Finni et al. (2018) demonstrated that Achilles subtendons have some ability to slide independently in Wistar rats (Finni et al., 2018). Maximum volitional ankle moments, electrically stimulated ankle moments and passive ankle moments are each significantly affected by ankle angle (Landin et al., 2015). Hug et al. (2013) and Liu et al. (2020) also reported significantly larger triceps surae MTU passive tension with ankle dorsiflexion compared with plantarflexion (Liu et al., 2020). Their findings suggested that a combination of differential triceps surae muscle loading, ankle angle and knee angle affected Achilles subtendon strain, magnitude of displacement and the magnitude of non-uniformity (i.e. differences in displacement between SOL and LG). Despite these findings, the anatomical differences between rats and humans may confound our interpretation of emergent subtendon tissue displacements. In addition, the Wistar rats were partially dissected to allow for sutures to be placed within the Achilles tendon potentially disrupting the *in situ* behavior of the muscle–subtendon units, which may affect the generalizability of the results. To our knowledge, no study to date has leveraged electrical muscle stimulation to regulate individual muscle activation while measuring the *in vivo* Achilles subtendon tissue response in human subjects.

The goal of this study was to leverage electrical muscle stimulation to quantify the effects of activation of individual triceps surae muscles on localized Achilles subtendon tissue displacements. Here, using electrical muscle stimulation to elicit a fixed-end contraction, we controlled the magnitude of longitudinal force transmitted through individual triceps surae muscle–subtendon units at various ankle angles and recorded the resultant Achilles subtendon displacements using ultrasound imaging. We hypothesized that electrical stimulation of individual triceps surae muscles would elicit larger displacements in their associated regions of the Achilles tendon. We also tested the secondary hypothesis that the relationship between individual and differential (SOL–MG) subtendon displacements would vary with ankle angle, which we would interpret in the context of MTU slack (Hug et al., 2013; Liu et al., 2020) and angle-dependent changes in passive tension (Davis et al., 2003; Landin et al., 2015).

MATERIALS AND METHODS

Subjects

Sixteen healthy young human subjects met our inclusion/exclusion criteria and provided written informed consent as per the University of North Carolina at Chapel Hill Institutional Review Board (16–0379). Participants had no musculoskeletal injuries over the previous 6 months and did not have a history of neuromuscular disease. We excluded six subjects during our quality control process for being unable to produce requisite peak ankle moments without discomfort elicited by electrical stimulation (n=2), protocol deviations that affected the prescribed ankle moment or analog synchronization (n=2), or poor ultrasound image quality (n=2). Thus, we report data for 10 subjects (age: 22.5±2.2 years, mass: 67.8±9.2 kg, height: 1.72±0.08 m, 7 females, 3 males).

Electrical stimulation equipment and protocol

Two DONECO stimulating electrodes (~50×50 mm with an interelectrode distance of 5 mm) were placed over the right leg muscle bellies of the MG and the posterolateral aspect of the SOL. Electrodes over both muscles were initially placed based on previous research methodologies (Stewart et al., 2007) and the anatomical motor point locations (Kim et al., 2005) before being repositioned on a subject-by-subject basis to elicit the largest twitch contraction under stimulation (Fig. 1). We aligned each pair of stimulating electrodes in the direction of the muscle fascicles (Hermens et al., 2000). Subjects first completed a 6 min warm-up walk on a treadmill (Bertec Corp., Columbus, OH, USA) at 1.2 m s^{-1} to precondition MTUs spanning their ankles (Hawkins et al., 2009).

Thereafter, subjects sat in a dynamometer (Biodex System 4 Pro, Biodex Medical Systems, Shirley, NY, USA) with their hip flexed to ~85 deg and knee flexed to 20 deg – the latter replicating the joint posture during the push-off phase of walking (Chao et al., 1983). Subjects then performed three maximum voluntary isometric contractions (MVICs) with their ankle at 20 deg plantarflexion. In pilot testing, this joint posture was determined to be the most uncomfortable during electrical stimulation, and thus ensured that subjects could cope with the stimulus intensities for all conditions. At this joint posture, we determined the stimulation intensities (i.e. $STIM_{MG}$ and $STIM_{SOL}$) necessary for the MG or SOL to produce 7.5% of the average peak net ankle moment generated from the three MVICs. We applied stimulation (Grass Instruments S48 Square Pulse Stimulator, A-M Systems, Carlsborg, WA, USA) using 11,300 µs pulses at 33 Hz according to published recommendations (Francis et al., 2013; Thelen et al., 2013). This frequency is thought to reduce subject discomfort while minimizing fatigue (Merletti et al., 1992). We chose 7.5% MVIC because this value produced a measurable net ankle moment (≥4 N m) without undue discomfort. We matched the desired ankle moment to preserve longitudinal force transmission through the Achilles tendon across all activations, thereby placing our interpretations in the context of constant force through the tendon, despite known differences in muscle force-generating capacity (Bojsen-Moller et al., 2010). In another condition, we prescribed simultaneous stimulation intensities (i.e. $STIM_{BOTH}$) that produced 15% MVIC peak net ankle moment (i.e. twice that of the individual muscles) with each individual muscle contributing 7.5% of the MVIC ankle moment. After all the trials were completed, the subjects then performed three MVICs again, which were later used to assess whether muscle fatigue occurred as a result of electrical stimulation.

After determining the voltages necessary to achieve 7.5% and 15% MVIC ankle moment, we maintained those voltages during all subsequent ankle angles. Specifically, at three ankle joint angles (i.e. 20 deg dorsiflexion, 0 deg 'neutral' and 20 deg plantarflexion), each subject underwent two contractions for three electrical stimulation activations: $STIM_{MG}$, $STIM_{SOL}$ and $STIM_{BOTH}$. In

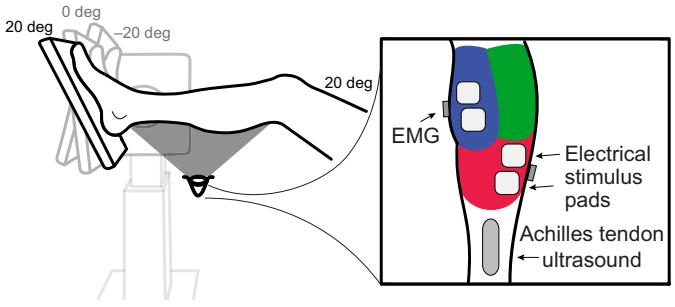

Fig. 1. Depiction of experimental setup illustrating a typical subject's right medial gastrocnemius (MG, blue), lateral gastrocnemius (green) and soleus (SOL, red). With the knee flexed to 20 deg, surface electrodes stimulated the MG and/or SOL muscles at three different ankle angles (20 deg plantarflexion, 0 deg and 20 deg dorsiflexion) while ultrasound recorded Achilles subtendon tissue displacements.

addition, subjects performed two volitional contractions (VOL) at each ankle angle using ankle moment biofeedback. Here, subjects volitionally matched the ankle moment generated by the dual stimulation activation using a screen positioned in front of the dynamometer that projected their instantaneous ankle moment and a target line representing the dual stimulation target moment (i.e. 15% MVIC). After a brief period of practice, subjects steadily increased their instantaneous ankle moment over 1 s, reached the target line, and then steadily returned to rest over 1 s. Between activations ($STIM_{MG}$, $STIM_{SOL}$, $STIM_{BOTH}$ and VOL), subjects rested for at least 1 min. We block randomized ankle angles and experimental activations as an additional measure to mitigate fatigue effects.

Electromyographic measurements

We placed wireless Delsys Trigno recording electrodes (Trigno, Delsys Inc., Natick, MA, USA) over the LG, MG and SOL muscle bellies near the stimulating electrodes and closest to Seniam recommendations (Hermens et al., 2000). During stimulation, we were unable to measure muscle activation via recording electrodes because of saturation, which occurred at ±2.5 V. Thus, we performed a low voltage sweep condition to estimate intermuscular excitation (e.g. $STIM_{MG}$ stimulating SOL muscle fibers) between the LG, MG and SOL. Specifically, we applied a continuous 300 µs pulse train at 33 Hz that gradually increased from 0 to 2.5 V. The low voltage sweep was applied to the MG and SOL at each ankle angle. We truncated and full wave rectified the measured LG, MG and SOL muscle activations between 0.75±0.05 and 2.25±0.05 V and segmented the ∼30 s collection into 250 ms blocks. Within each block, we determined the activation ratios between the LG, MG and SOL by comparing peak EMG values. For each muscle being stimulated (i.e. MG and SOL), Pearson's correlation coefficients determined the relation between stimulation intensity (i.e. voltage) and measured activation ratios.

Ultrasound measurements

A 7 MHz 38 mm linear array ultrasound transducer (L14-5W/38, Ultrasonix Corporation, Richmond, BC, Canada) operating at 155 frames s^{-1} recorded 128 lines of ultrasound radiofrequency data from subjects' right free Achilles tendon. The transducer was placed ∼6 cm proximal to the calcaneal insertion and was secured via a custom orthotic (Franz et al., 2015). A two-dimensional (2D) speckle tracking algorithm estimated localized displacements of Achilles tendon tissue using previously published techniques (Chernak and Thelen, 2012; Chernak Slane and Thelen, 2014). In brief, we placed a rectangular region of interest ∼15×3 mm on a B-mode ultrasound image of the free Achilles tendon at rest. The region of interest contained a grid of nodes with 0.83×0.42 mm spacing defined to encompass only tendinous tissue. A 2×1 mm kernel containing up-sampled (4×) radiofrequency data, centered at each nodal position, provided a search window over which we defined 2D normalized cross-correlation functions between successive frames. We defined localized frame-to-frame nodal displacements that maximized these 2D cross-correlations, with the cumulative displacement representing the average of forward and backward tracking results. Subtendon tissue displacements were determined by averaging the displacements of nodes arising from two equally sized tendon depths, deep and superficial, corresponding to the part of the Achilles anatomically considered to originate from the SOL and MG, respectively. Although many studies have acknowledged variation in Achilles tendon architecture, our reported orientation, with equal-sized MG and SOL subtendons, represents the majority of anatomical observations in cadaveric studies (Del Buono et al., 2013; Edama et al., 2015; Szaro et al., 2009; van Gils et al., 1996).

Data reduction and analysis

We filtered peak ankle moment and subtendon displacement data using a fourth-order Butterworth low-pass filter with a cut-off frequency of 12 Hz. Binary analog signals originating from the ultrasound and Grass stimulator were used to synchronize ultrasound imaging with stimulation onset and ankle moment generation. We analyzed all data between 'key-frames' signifying the start and end of the trial. For the volitional condition, key-frames represented the onset and offset of ankle moment generation using a 5% threshold based on that condition's peak value. For the electrical stimulation conditions, the start key-frame represented the onset of stimulation and the end key-frame used an analogous 5% threshold. From there, we report data measures of the peak of the filtered data within this time window.

Statistical analysis

Statistical analyses were performed using SPSS Statistics 26 (SPSS, Chicago, IL, USA). First, we extracted peak values then averaged the two trials of each experimental condition for each subject. We then performed two 2-way (activation×ankle angle) repeated-measures ANOVAs, with one ANOVA containing individual stimulation conditions ($STIM_{MG}$ and $STIM_{SOL}$) and one ANOVA containing the remaining conditions ($STIM_{BOTH}$ and VOL) for each of the following primary outcome measures: peak ankle moment, peak SOL subtendon displacement, peak MG subtendon displacement and Achilles tendon non-uniformity (i.e. peak SOL subtendon displacement – peak MG subtendon displacement) during experimental conditions. In addition, we performed a three-way ANOVA (ankle angle×activation×MG and SOL subtendon displacement) on individual displacement to assess whether there were significant differences between MG and SOL displacement patterns. We also performed a one-way (ankle angle) repeated-measures ANOVA on passive ankle moment. When a significant main effect or interaction was found, we performed *post hoc* *t*-tests with Bonferroni corrections to assess differences between activations at each ankle angle. When a significant interaction effect was found, we selectively used *post hoc* ANOVAs to examine any potentially insightful main effects of ankle angle on a particular activation. Effect sizes are reported as η_p^2 and Cohen's *d* for main effects and pairwise comparisons, respectively.

We used a combination of two mixed models to determine whether generated ankle moment was a governing factor in measured tendon non-uniformity. We used a generalized linear mixed model with activation and ankle angle as fixed factors and generated moment as a random factor. In addition, we used a linear mixed model to estimate effect sizes of fixed and random factors. One-sided paired Student's *t*-tests were performed to determine whether there was fatigue owing to electrical stimulation by testing whether subject's averaged post-collection MVIC was less than their averaged pre-collection MVIC. One-sample *t*-tests also determined whether EMG activation ratios were preserved across a range of stimulation voltages by comparing Pearson's correlation coefficients of activation ratios (MG/LG/SOL) with 0. Bonferroni-corrected *t*-tests used an alpha level of 0.0083 (i.e. 0.05/6). For all other comparisons, we defined significance using an alpha level of 0.05.

RESULTS

All results are reported as means±s.d. Muscle stimulation was largely preserved to the muscle of interest; activation ratios during

Journal of Experimental Biology (2021) 224, jeb242135. doi:10.1242/jeb.242135

the low-voltage sweep averaged 13.4:1 (MG:SOL) for $STIM_{MG}$ and 11.7:1 (SOL:MG) for $STIM_{SOL}$, and the slope of the relationship between activation ratio and voltage was not significantly different from 0 ($P \geq 0.190$).

Peak ankle moment

We found no difference between baseline MVIC moments (81.3±29.6 N m) and those measured at the end of the session (73.2±22.2 N m) ($P=0.194$). We observed a significant main effect of ankle angle on passive ankle moment ($F_{1,11}=18.073$, $P<0.001$, $\eta_P^2=0.668$), with significant pairwise comparisons revealing increases from 20 deg plantarflexion to 20 deg dorsiflexion ($P \leq 0.036$, $d \geq 0.441$; Fig. 2). However, when comparing $STIM_{MG}$ and $STIM_{SOL}$, we did not observe a significant main effect of ankle angle ($F_{2,18}=1.931$, $P=0.174$, $\eta_P^2=0.177$), a significant main effect of activation ($F_{1,9}=0.947$, $P=0.356$, $\eta_P^2=0.095$) or a significant angle×activation interaction effect ($F_{2,18}=1.556$, $P=0.238$, $\eta_P^2=0.147$) on peak ankle moment. Likewise, when comparing $STIM_{BOTH}$ and VOL activations, we did not observe a significant main effect of ankle angle ($F_{2,16}=2.032$, $P=0.163$, $\eta_P^2=0.203$), a significant effect of activation ($F_{1,8}=0.106$, $P=0.753$, $\eta_P^2=0.013$) or a significant angle×activation interaction effect ($F_{2,6}=2.640$, $P=0.102$, $\eta_P^2=0.248$) on peak ankle moment (Fig. 3A).

Individual subtendon tissue displacements

For $STIM_{MG}$ and $STIM_{SOL}$ conditions, we observed a significant main effect of ankle angle (MG: $F_{1,11}=8.943$, $P=0.009$, $\eta_P^2=0.498$; SOL: $F_{1,12}=11.776$, $P=0.003$, $\eta_P^2=0.567$) on individual subtendon displacements. However, we did not observe a significant main effect of activation (MG: $F_{1,9}=0.839$, $P=0.384$, $\eta_P^2=0.085$; SOL: $F_{1,9}=0.168$, $P=0.692$, $\eta_P^2=0.018$) or an angle×activation interaction effect (MG: $F_{1,10}=0.069$, $P=0.839$, $\eta_P^2=0.008$; SOL: $F_{2,18}=0.989$, $P=0.391$, $\eta_P^2=0.099$) on individual subtendon displacements (Fig. 3B). Independent of ankle angle, we observed no significant pairwise difference between individual stimulation condition (i.e. $STIM_{MG}$ versus $STIM_{SOL}$) on MG subtendon or SOL subtendon displacement ($P \geq 0.495$, $d \leq 0.319$). For $STIM_{BOTH}$ and VOL conditions, we observed a significant main effect of ankle angle (MG: $F_{2,16}=14.293$, $P=0.001$, $\eta_P^2=0.641$; SOL: $F_{2,16}=22.118$, $P<0.001$, $\eta_P^2=0.734$), a significant main effect of activation ($F_{1,8}=10.832$, $P=0.011$, $\eta_P^2=0.575$; SOL: $F_{1,8}=20.576$, $P=0.002$, $\eta_P^2=0.720$) and a significant angle×activation interaction effect (MG: $F_{1,10}=8.034$, $P=0.014$, $\eta_P^2=0.501$; SOL: $F_{2,16}=15.769$, $P<0.001$, $\eta_P^2=0.663$) on individual subtendon displacement. Pairwise comparisons revealed significantly larger SOL subtendon displacements for $STIM_{BOTH}$ compared with volitional activations at 20 deg plantarflexion ($P=0.012$, $d=1.641$) (Fig. 3B). Group average subtendon displacement profiles are shown in Fig. 4.

For the three-way ANOVA, we observed a significant main effect of ankle angle ($F_{2,16}=20.170$, $P<0.001$, $\eta_P^2=0.716$), a significant main effect of activation ($F_{3,24}=9.581$, $P<0.001$, $\eta_P^2=0.545$), a significant main effect of MG/SOL subtendon displacement ($F_{1,8}=29.778$, $P=0.001$, $\eta_P^2=0.788$) and a significant angle×activation×subtendon interaction effect ($F_{2,19}=4.042$, $P=0.028$, $\eta_P^2=0.336$). We observed significantly larger SOL subtendon displacement compared with MG subtendon displacement at 20 deg plantarflexion under $STIM_{SOL}$ and $STIM_{BOTH}$, at a neutral ankle angle under $STIM_{SOL}$, $STIM_{BOTH}$ and VOL activation, and at 20 deg dorsiflexion under VOL activation ($P \leq 0.024$, $d \geq 0.761$), as shown in Fig. 3B.

Achilles tendon tissue non-uniformity

For $STIM_{MG}$ and $STIM_{SOL}$ activations, we did not observe a main effect of ankle angle ($F_{2,18}=2.908$, $P=0.080$, $\eta_P^2=0.244$) on the magnitude of Achilles tendon tissue non-uniformity. However, we observed a significant main effect of activation ($F_{1,9}=5.901$, $P=0.038$, $\eta_P^2=0.396$) and a significant activation×angle interaction effect ($F_{2,18}=6.889$, $P=0.006$, $\eta_P^2=0.434$) on Achilles tendon non-uniformity (Fig. 3C). For $STIM_{SOL}$, a one-way *post hoc* ANOVA revealed a significant main effect of ankle angle ($F_{2,17}=8.280$, $P=0.009$, $\eta_P^2=0.479$) on Achilles tendon non-uniformity. For $STIM_{MG}$, a one-way *post hoc* ANOVA revealed no significant main effect of ankle angle ($F_{2,17}=0.582$, $P=1.000$, $\eta_P^2=0.061$) on Achilles tendon non-uniformity. At 20 deg plantarflexion, pairwise comparisons revealed significantly larger Achilles tendon non-uniformity arising from $STIM_{SOL}$ versus $STIM_{MG}$ ($P=0.024$, $d=0.871$, Fig. 3C). For $STIM_{BOTH}$ and volitional activations, we observed a significant main effect of ankle angle ($F_{2,16}=4.161$, $P=0.035$, $\eta_P^2=0.342$). However, we observed no main effect of activation ($F_{1,8}=3.134$, $P=0.115$, $\eta_P^2=0.281$), nor a significant activation×angle interaction effect ($F_{2,16}=1.186$, $P=0.331$, $\eta_P^2=0.129$) on Achilles tendon tissue non-uniformity. Group average Achilles tendon non-uniformity displacement profiles are shown in Fig. 5.

Using the generalized linear mixed model, we did not observe an effect of peak moment on tendon non-uniformity ($P=0.092$). Moreover, a linear mixed model yielded larger estimated effect sizes (f^2) for fixed factors (activation and ankle angle; $f^2=0.500\pm0.051$, $P<0.001$) compared with the random factor (peak moment; $f^2=0.310\pm0.040$).

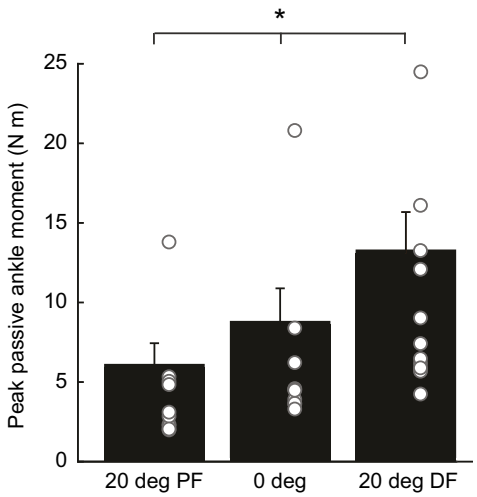

Fig. 2. Group mean (±s.e.m.; *n*=10) peak passive ankle moment for each ankle angle [20 deg plantarflexion (PF), 0 deg and 20 deg dorsiflexion (DF)]. Individual data points are represented by open gray circles. Asterisk (*) represents a significant difference between ankle angles ($P<0.0083$).

DISCUSSION

In this study, we quantified the effects of triceps surae (i.e. SOL, MG) muscle activation on localized Achilles subtendon displacement patterns using targeted electrical muscle stimulation and ultrasound imaging. Moreover, we controlled for peak ankle moment between analogous activations (i.e. $STIM_{MG}$ versus $STIM_{SOL}$ and $STIM_{BOTH}$ versus VOL) to preserve longitudinal force transmission through the Achilles tendon, thereby placing our interpretations in the context of constant longitudinal force

Journal of Experimental Biology (2021) 224, jeb242135. doi:10.1242/jeb.242135

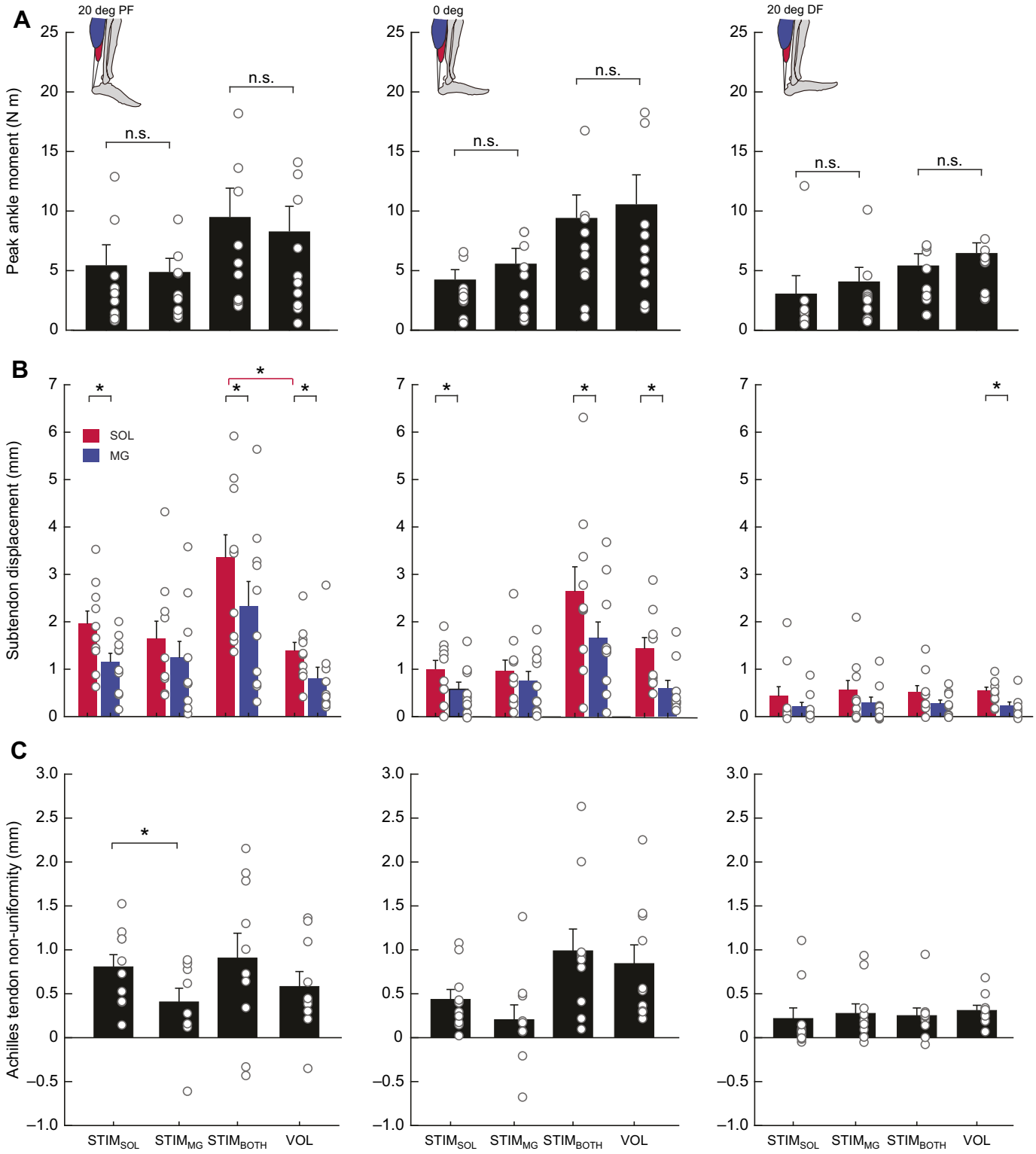

Fig. 3. Group mean (±s.e.m.) peak ankle moment, peak individual subtendon displacement and peak Achilles tendon non-uniformity for each experimental activation at each ankle angle. Individual data points (n=10) are represented by open gray circles. (A) For peak ankle moment, consistent with our experimental design, non-significant differences between experimental activations with similar ankle moment targets ($STIM_{MG}$ versus $STIM_{SOL}$ and $STIM_{BOTH}$ versus VOL) are denoted as brackets labeled n.s. (P>0.05). (B) For peak individual subtendon displacement, brackets with asterisks (*) represent significant differences between stimulation activations for the SOL subtendon (red), MG (blue) or between subtendons (black) (P<0.0083). (C) For peak Achilles tendon non-uniformity, brackets with asterisks (*) represent significant differences between stimulation activations (black) (P<0.0083).

transmission despite known differences in muscle force-generating capacity (Fukunaga et al., 1996; Kinugasa et al., 2005). Together, this paradigm provides an important step toward evaluating a relationship between muscle activation and non-uniform displacement patterns within the Achilles tendon. Our tendon tissue-level responses were more complex than anticipated.

Journal of Experimental Biology (2021) 224, jeb242135. doi:10.1242/jeb.242135

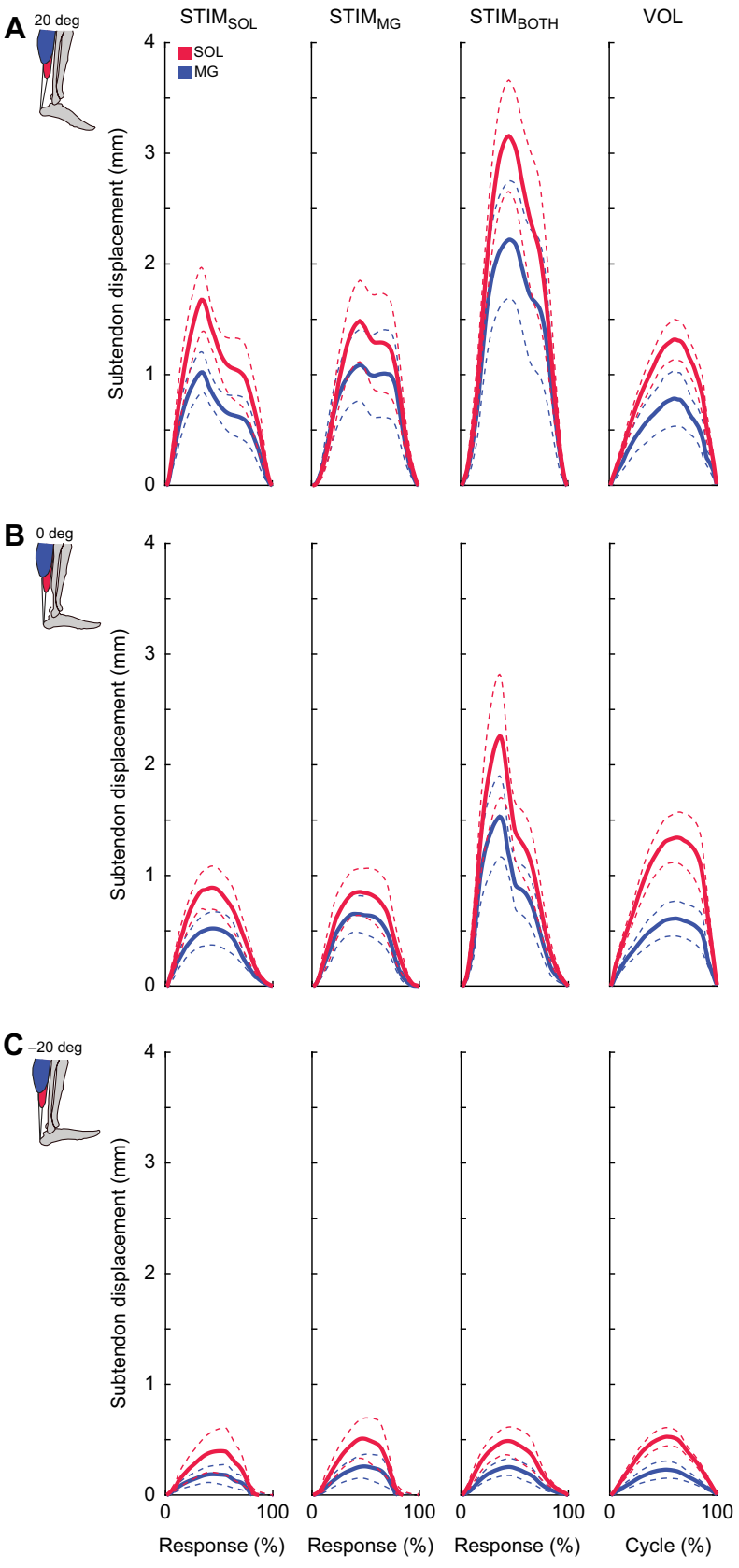

Fig. 4. Time-normalized group mean (±s.e.m.) displacement patterns (*n*=10) for the MG subtendon (blue) and SOL subtendon (red) for each experimental activation. (A) 20 deg plantarflexion, (B) 0 deg neutral ankle angle and (C) 20 deg dorsiflexion.

Nevertheless, in partial support of our first hypothesis, SOL and MG subtendon tissue displacements exhibited what we interpret to be anatomically consistent responses to electrical stimulation of individual triceps surae muscles, at least when the ankle was in plantarflexion. In this context, anatomical consistence presents itself in two main ways: Achilles tendon non-uniformity is larger under STIM$_{SOL}$ compared with STIM$_{MG}$, and we observe larger displacements in the stimulated subtendon relative to the condition

Journal of Experimental Biology (2021) 224, jeb242135. doi:10.1242/jeb.242135

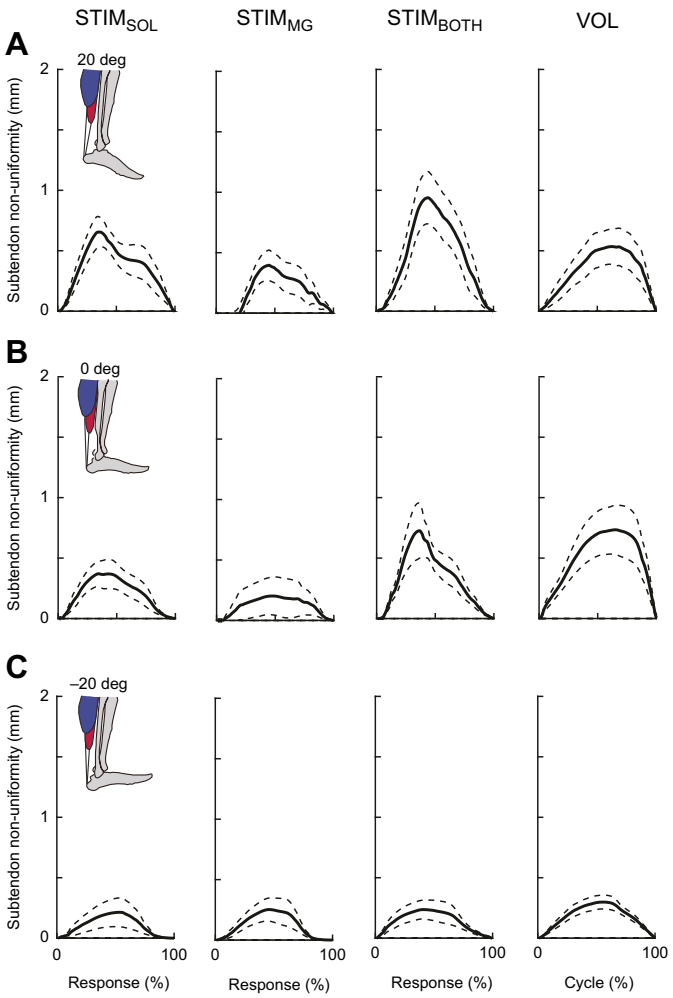

Fig. 5. Time-normalized group mean (s.e.m.) displacement patterns (*n*=10) for the magnitude of Achilles tendon tissue non-uniformity (SOL–MG subtendon displacement) for each experimental activation. (A) 20 deg plantarflexion, (B) 0 deg neutral ankle angle and (C) 20 deg dorsiflexion. Here, positive *y*-axis values indicate greater SOL subtendon tissue displacement relative to MG subtendon tissue displacement.

where it is not stimulated (i.e. SOL subtendon displacement is larger under STIM$_{SOL}$ than under STIM$_{MG}$). Specifically, despite no difference in net longitudinal force transmitted via the Achilles tendon, STIM$_{SOL}$ elicited much larger SOL subtendon tissue displacements than those in response to STIM$_{MG}$ in plantarflexion. Moreover, in support of our second hypothesis, SOL and MG subtendon tissue displacement were sensitive to ankle angle, with smaller magnitudes of displacements in angles associated with greater passive tension (i.e. largest displacements in plantarflexion and smallest displacements in dorsiflexion). In addition, *post hoc* one-way ANOVAs revealed that Achilles tendon non-uniformity (SOL–MG subtendon displacement) was only sensitive to changes in ankle angle during STIM$_{SOL}$ activations. As we elaborate below, these findings point to at least some mechanical independence in actuation between the human triceps surae MTUs, which warrants further study.

In this study, we sought empirical data associated with the relative independence of triceps surae muscle–subtendon units in response to muscle stimulation during fixed-end contractions. Interestingly, independent of angle or activation, SOL subtendon tissue displaced, on average, more than MG subtendon tissue. Larger relative tissue displacements in the SOL subtendon are most likely multifactorial in nature. For example, such behavior may arise from differences between LG, MG and SOL muscle and/or subtendon tissue morphology or mechanical properties. At the muscle level, the human SOL has far greater force-generating capacity than the MG and LG (Albracht et al., 2008), and exhibits greater fascicle shortening and rotation during muscle action (Clark and Franz, 2018). Likely as a result, in a similar study using electrical stimulation on rat MTUs at similar knee angles, Maas et al. (2020) observed greater LG subtendon displacement than SOL subtendon displacement only when both biarticular gastrocnemius muscles were stimulated (Maas et al., 2020). Moreover, differences in mechanical properties (e.g. stiffness) are a plausible determinant for consistently larger displacements in the SOL subtendon. Using electrical stimulation in an animal model, Finni et al. (2018) found that the SOL subtendon undergoes greater strain during SOL muscle stimulation (8.4%) compared with the LG subtendon under equivalent LG muscle stimulation (4.7%). The authors attribute the differences in subtendon strain arising from isolated activation to differences in subtendon stiffness; namely, that the SOL subtendon is more compliant than its LG counterpart (Finni et al., 2018). During LG stimulation, those authors observed equal displacements in SOL and LG subtendons. In agreement with the findings from Finni and colleagues (2018), Ekiert et al. (2021) determined that the SOL subtendon has a significantly lower (approximately 25%) tensile modulus than the MG subtendon in the Achilles tendon of human cadavers (Ekiert et al., 2021). Likely as a result, in contrast to disparate responses during SOL stimulation, we observed indistinguishable tissue displacements in the SOL and MG subtendons during MG stimulation. However, these differences are unlikely to fully explain our findings, particularly for activations designed for isolated MG stimulation, where our results could indicate that we are also observing lateral force transmission between muscle–subtendon units. As yet an additional explanation, the interfascicular matrix of the Achilles tendon unevenly distributes forces between adjacent subtendons (Gains et al., 2020), with possible preference for the more compliant SOL subtendon in order to reduce the risk of injury. Thorpe et al. (2015, 2016) have shown that the interfascicular matrix is able to withstand considerable loading and that it may have different mechanical properties in different tendons (Thorpe et al., 2015, 2016). Although not unanticipated, we cannot presume complete independence in actuation between triceps surae MTUs. However, as noted by Tian et al. (2012), lateral force transmission in the human Achilles tendon is small.

Despite consistently larger tissue displacements in the SOL subtendon, variations in tendon non-uniformity (i.e. SOL subtendon – MG subtendon) were sensitive to individual stimulation activation and ankle angle. On average, during individual muscle stimulation activations (i.e. STIM$_{SOL}$ and STIM$_{MG}$), Achilles tendon non-uniformity decreased (–61%) from plantarflexion to dorsiflexion. However, a significant activation×angle interaction effect suggests that this was driven by the STIM$_{SOL}$ activation; the magnitude of Achilles tendon non-uniformity during STIM$_{MG}$ was independent of ankle angle. At 20 deg dorsiflexion, we did not observe significant differences between any stimulation activations, likely because of an increase in passive tension and thus a reduce capacity for tendon tissue motion. Using shear wave elastography, Hug et al. (2013) reported larger triceps surae MTU passive tension with ankle dorsiflexion (Hug et al., 2013). Moreover, Liu et al. (2020) reported up to 4-fold increase in triceps surae MTU stiffness as the ankle moves from plantarflexion to dorsiflexion (Liu et al., 2020). Perhaps

accordingly, we found no $STIM_{MG}$ versus $STIM_{SOL}$ effects on tendon non-uniformity at 0 deg (i.e. neutral) or 20 deg dorsiflexion. An increase in MTU stiffness, presumably the result of increased passive tension, would yield smaller subtendon tissue displacements for the same level of longitudinal force transmission, consistent with our observations.

Conversely, when subtendon tissue displacements were largest and passive tension smallest (i.e. 20 deg plantarflexion), $STIM_{SOL}$ elicited significantly larger (+49%) tendon non-uniformity than did $STIM_{MG}$. Although it was positive for all conditions, the magnitude of non-uniformity varied in anatomically consistent ways in response to individual triceps surae muscle activation at 20 deg plantarflexion. Previously, Clark and Franz (2018) observed a positive correlation between differences in MG and SOL muscle shortening and non-uniform Achilles tendon tissue displacements during maximum isometric contractions (Clark and Franz, 2018). They interpreted their results to suggest that triceps surae muscle dynamics may precipitate non-uniform displacement patterns. However, both the MG and SOL were simultaneously and maximally activated in their experimental design and thus the conclusions could be influenced by differences in force-generating capacities and neuromuscular control. In contrast, our findings control for these confounding factors and add *in vivo* evidence of at least some mechanical independence in actuation between the human triceps surae MTUs – with potential implications for muscle–tendon function during walking. Indeed, many studies suggest that the gastrocnemius and SOL muscles contribute in biomechanically different ways to powering locomotion – evidenced by different changes in activation (Clark et al., 2020; Gottschall and Kram, 2003; Miyoshi et al., 2006) and fascicle length (Clark et al., 2020; Cronin et al., 2013) in response to altered task demand, which may be an indication of at least some level of independence between the Achilles subtendons. Some level of mechanical independence between triceps surae MTUs may be advantageous by allowing the biarticular gastrocnemius and uniarticular SOL to adopt unique patterns of actuation and contribute in different ways to forward propulsion and vertical support (Francis et al., 2013; Gottschall and Kram, 2003; Lenhart et al., 2014). Alternatively, lateral force transmission may reduce peak stresses and thereby reduce risk of tendon injury (Maas and Finni, 2018).

Although necessary to abate subject discomfort, the prescribed ankle moment in our study of 7.5% and 15% of subjects' MVIC may not be representative of physiological loading during functional activity. Very recently, during volitional plantarflexion tasks, Wolfram et al. (2020) observed tendon non-uniformity only after subjects reached 30% of their MVIC moment (Wolfram et al., 2020). However, they only examined non-uniformity between the LG and MG and used muscle–tendon junction kinematics which may not be representative of Achilles subtendon tissue displacements owing to unaccounted-for anatomical complexity distal to the muscle–tendon junction (DeWall et al., 2014). Nevertheless, it is plausible that our study's prescription of longitudinal force transmission, less than that generally expected during physiological loading, may prevent definitive extrapolations to more functional activities such as walking. Indeed, peak moment values during walking average roughly 60 to 166 N m depending on walking speed (Hof et al., 2002), at least five times higher than our values (<11 N m) during $STIM_{SOL}$ and $STIM_{MG}$ activations. Compared with the relatively low peak ankle moments prescribed in our study design, we suspect that individual SOL versus MG stimulation would have larger disparate effects on tendon non-uniformity at higher levels of force generation, independent of ankle angle – an important caveat in the translational of our findings to walking.

Establishing a baseline understanding of the relationship between individual triceps surae muscle activation and resultant Achilles subtendon displacement patterns has important implications for the study of gait and mobility limitations. For example, we recently revealed that older adults have more uniform subtendon tissue displacements during MVIC tasks that extend to more uniform muscle fascicle displacement patterns and potentially unfavorable changes in muscle contractile behavior (Clark and Franz, 2020). Also, Thorpe et al. (2015, 2016) have observed that the interfascicular matrix of animals becomes stiffer with increasing age, which may also play a critical role in changing subtendon displacement patterns (Thorpe et al., 2015, 2016). In addition, electrical stimulation could elucidate age-related mechanism by which (i) muscle-level behavior is inhibited by tendon-level behavior (via interfascicle adhesions and collagen crosslinking) (Narici et al., 2008) or (ii) tendon-level behavior is inhibited by muscle-level behavior (via changes in protein biology and muscle coordination, and loss of viable motor units) (Miller et al., 2014). This research may be crucial in developing intervention techniques and diagnostic tools to help improve older adults' quality of life and well-being. As another example, better procedures could be devised for surgically repairing ruptured Achilles tendons or in response to other tendon injuries.

Limitations

There are several limitations of this study. First, we only matched activation ratios between stimulation activations at 20 deg plantarflexion. However, we did not observe any significant differences between peak moment of similar activations (i.e. $STIM_{MG}$ versus $STIM_{SOL}$ and $STIM_{BOTH}$ versus VOL) at any ankle angle. Second, we only report isolated stimulation of the MG and SOL, along with a generalized approximation of the anatomical structure of the MG and SOL subtendons. This approximation represents the most common variation of Achilles tendon anatomy, though variations with differing magnitudes of Achilles tendon twist exist and would necessarily impact our interpretations (Edama et al., 2015; Szaro et al., 2009; van Gils et al., 1996). Third, our 2D ultrasound imaging technique does not fully capture the complex 3D motion of the Achilles tendon, which could lead to underestimating or overestimating gross subtendon tissue displacements. Likewise, we have previously described the limitations of the 2D speckle-tracking estimates of Achilles subtendon displacements (Clark and Franz, 2018; Franz et al., 2015). Fourth, we cannot ensure isolated stimulation of the intended muscle (MG/SOL) because of the nature of surface stimulating electrodes and EMG saturation. We have presented activation ratios of 13.4:1 (MG:SOL) for $STIM_{MG}$ and 11.7:1 (SOL:MG) for $STIM_{SOL}$ at intensities below that which elicited EMG saturation. Over the 0–5 V range which we could measure this ratio, we observed no significant change in activation ratios. Although this ratio may have decreased during experimental conditions, we suggest that more uniform stimulation would be most likely to yield more uniform displacement patterns. Accordingly, the measurable non-uniformity in tendon tissue displacements we observed are at least representative of a limited distribution of electrical stimulation to neighboring muscles. Fifth, researchers have demonstrated lateral force transmission between adjacent triceps surae muscle bellies (Bernabei et al., 2015; Bojsen-Moller et al., 2010; Tian et al., 2012) that can increase with increased muscle activation (Finni et al.,

2017; Tijs et al., 2016). These complex mechanics of intermuscular lateral force transmission may make drawing concrete conclusions difficult. However, because we controlled for the magnitude of longitudinal force transmission between experimental conditions with similar ankle moment targets ($STIM_{MG}$ versus $STIM_{SOL}$ and $STIM_{BOTH}$ versus VOL), it is likely that the effect of lateral force transmission between subtendons would be similar and thus would not affect our interpretation. Sixth, we note that during experimental conditions, ankle angle may have shifted slightly. A kinematic analysis of motion capture from a subset of subjects revealed peak ankle angles changes of 0.94±1.24 deg for individual simulation activations and 0.86±0.89 deg for $STIM_{BOTH}$ and VOL activations. However, these changes in ankle angle likely had negligible effects on tendon tissue displacements owing to the low level of elicited peak ankle moment (<11 N m). Finally, our relatively small sample size may contribute to an underpowered statistical assessment and increase the risk of a type II error.

Conclusions

Our results suggest that localized tissue displacements within the architecturally complex Achilles tendon respond in anatomically consistent ways to different patterns of triceps surae muscle activation, with early evidence here at 20 deg plantarflexion at relatively low force levels, and that the relationship is highly susceptible to changes in ankle joint angle. Accordingly, this *in vivo* evidence points to at least some mechanical independence in actuation between the human triceps surae muscle–subtendon units. Our research may be important in establishing a baseline of individual triceps surae muscle contributions to subtendon displacement patterns that will facilitate a deeper understanding of deleterious changes owing to aging, tendon injury or surgical intervention, which may have important implications in the design and implementation of clinical interventions to improve tendon health and preserve/restore mobility.

Competing interests

The authors declare no competing or financial interests.

Author contributions

Conceptualization: N.L.L., W.H.C., J.R.F.; Software: J.R.F.; Validation: N.L.L., W.H.C., J.R.F.; Formal analysis: W.H.C., J.R.F.; Investigation: N.L.L., W.H.C., M.D.L., J.R.F.; Writing - original draft: N.L.L., W.H.C., M.D.L., J.R.F.

Funding

This research was supported by grants from the National Institutes of Health (R01AG051748, F31AG060675) and by the UNC–NC State Joint Department of Biomedical Engineering Lucas Scholar Fellowship. The funders had no role in study design, data collection and analysis, decision to publish, or preparation of the manuscript. Deposited in PMC for release after 12 months.

References

Albracht, K., Arampatzis, A. and Baltzopoulos, V. (2008). Assessment of muscle volume and physiological cross-sectional area of the human triceps surae muscle *in vivo*. *J. Biomech.* **41**, 2211-2218. doi:10.1016/j.jbiomech.2008.04.020

Arndt, A., Bengtsson, A. S., Peolsson, M., Thorstensson, A. and Movin, T. (2012). Non-uniform displacement within the Achilles tendon during passive ankle joint motion. *Knee Surg. Sports Traumatol. Arthrosc.* **20**, 1868-1874. doi:10.1007/s00167-011-1801-9

Bernabei, M., Van Dieen, J. H., Baan, G. C. and Maas, H. (2015). Significant mechanical interactions at physiological lengths and relative positions of rat plantar flexors. *J. Appl. Physiol.* **118**, 427-436. doi:10.1152/japplphysiol.00703.2014

Bojsen-Moller, J., Schwartz, S., Kalliokoski, K. K., Finni, T. and Magnusson, S. P. (2010). Intermuscular force transmission between human plantarflexor muscles in vivo. *J. Appl. Physiol.* **109**, 1608-1618. doi:10.1152/japplphysiol.01381.2009

Chao, E. Y., Laughman, R. K., Schneider, E. and Stauffer, R. N. (1983). Normative data of knee joint motion and ground reaction forces in adult level walking. *J. Biomech.* **16**, 219-233. doi:10.1016/0021-9290(83)90129-X

Chernak, L. A. and Thelen, D. G. (2012). Tendon motion and strain patterns evaluated with two-dimensional ultrasound elastography. *J. Biomech.* **45**, 2618-2623. doi:10.1016/j.jbiomech.2012.08.001

Chernak Slane, L. and Thelen, D. G. (2014). The use of 2D ultrasound elastography for measuring tendon motion and strain. *J. Biomech.* **47**, 750-754. doi:10.1016/j.jbiomech.2013.11.023

Clark, W. H. and Franz, J. R. (2018). Do triceps surae muscle dynamics govern non-uniform Achilles tendon deformations? *PeerJ* **6**, e5182. doi:10.7717/peerj.5182

Clark, W. H. and Franz, J. R. (2020). Triceps surae muscle-subtendon interaction differs between young and older adults. *Connect. Tissue Res.* **61**, 104-113. doi:10.1080/03008207.2019.1612384

Clark, W. H., Pimentel, R. E. and Franz, J. R. (2020). Imaging and Simulation of inter-muscular differences in triceps surae contributions to forward propulsion during walking. *Ann. Biomed. Eng.* **49**, 703-715.

Cronin, N. J., Avela, J., Finni, T. and Peltonen, J. (2013). Differences in contractile behaviour between the soleus and medial gastrocnemius muscles during human walking. *J. Exp. Biol.* **216**, 909-914. doi:10.1242/jeb.078196

Davis, J., Kaufman, K. R. and Lieber, R. L. (2003). Correlation between active and passive isometric force and intramuscular pressure in the isolated rabbit tibialis anterior muscle. *J. Biomech.* **36**, 505-512. doi:10.1016/S0021-9290(02)00430-X

Del Buono, A., Chan, O. and Maffulli, N. (2013). Achilles tendon: functional anatomy and novel emerging models of imaging classification. *Int. Orthop.* **37**, 715-721. doi:10.1007/s00264-012-1743-y

Dewall, R. J., Slane, L. C., Lee, K. S. and Thelen, D. G. (2014). Spatial variations in Achilles tendon shear wave speed. *J. Biomech.* **47**, 2685-2692. doi:10.1016/j.jbiomech.2014.05.008

Edama, M., Kubo, M., Onishi, H., Takabayashi, T., Inai, T., Yokoyama, E., Hiroshi, W., Satoshi, N. and Kageyama, I. (2015). The twisted structure of the human Achilles tendon. *Scand. J. Med. Sci. Sports* **25**, e497-e503. doi:10.1111/sms.12342

Ekiert, M., Tomaszewski, K. A. and Mlyniec, A. (2021). The differences in viscoelastic properties of subtendons result from the anatomical tripartite structure of human Achilles tendon – *ex vivo* experimental study and modeling. *Acta Biomater.* **125**, 138-153. doi:10.1016/j.actbio.2021.02.041

Farris, D. J. and Sawicki, G. S. (2012). The mechanics and energetics of human walking and running: a joint level perspective. *J. R Soc. Interface* **9**, 110-118. doi:10.1098/rsif.2011.0182

Finni, T., Cronin, N. J., Mayfield, D., Lichtwark, G. A. and Cresswell, A. G. (2017). Effects of muscle activation on shear between human soleus and gastrocnemius muscles. *Scand. J. Med. Sci. Sports* **27**, 26-34. doi:10.1111/sms.12615

Finni, T., Bernabei, M., Baan, G. C., Noort, W., Tijs, C. and Maas, H. (2018). Non-uniform displacement and strain between the soleus and gastrocnemius subtendons of rat Achilles tendon. *Scand. J. Med. Sci. Sports* **28**, 1009-1017. doi:10.1111/sms.13001

Francis, C. A., Lenz, A. L., Lenhart, R. L. and Thelen, D. G. (2013). The modulation of forward propulsion, vertical support, and center of pressure by the plantarflexors during human walking. *Gait Posture* **38**, 993-997. doi:10.1016/j.gaitpost.2013.05.009

Franz, J. R. and Thelen, D. G. (2015). Depth-dependent variations in Achilles tendon deformations with age are associated with reduced plantarflexor performance during walking. *J. Appl. Physiol.* **119**, 242-249. doi:10.1152/japplphysiol.00114.2015

Franz, J. R., Slane, L. C., Rasske, K. and Thelen, D. G. (2015). Non-uniform in vivo deformations of the human Achilles tendon during walking. *Gait Posture* **41**, 192-197. doi:10.1016/j.gaitpost.2014.10.001

Fukunaga, T., Roy, R. R., Shellock, F. G., Hodgson, J. A. and Edgerton, V. R. (1996). Specific tension of human plantar flexors and dorsiflexors. *J. Appl. Physiol.* **80**, 158-165. doi:10.1152/jappl.1996.80.1.158

Gains, C. C., Correia, J. C., Baan, G. C., Noort, W., Screen, H. R. C. and Maas, H. (2020). Force transmission between the gastrocnemius and soleus sub-tendons of the Achilles tendon in rat. *Front. Bioeng. Biotechnol.* **8**, 700. doi:10.3389/fbioe.2020.00700

Gottschall, J. S. and Kram, R. (2003). Energy cost and muscular activity required for propulsion during walking. *J. Appl. Physiol. (1985)* **94**, 1766-1772. doi:10.1152/japplphysiol.00670.2002

Hawkins, D., Lum, C., Gaydos, D. and Dunning, R. (2009). Dynamic creep and pre-conditioning of the Achilles tendon *in-vivo*. *J. Biomech.* **42**, 2813-2817. doi:10.1016/j.jbiomech.2009.08.023

Hermens, H. J., Freriks, B., Disselhorst-Klug, C. and Rau, G. (2000). Development of recommendations for SEMG sensors and sensor placement procedures. *J. Electromyogr. Kinesiol.* **10**, 361-374. doi:10.1016/S1050-6411(00)00027-4

Hof, A. L., Van Zandwijk, J. P. and Bobbert, M. F. (2002). Mechanics of human triceps surae muscle in walking, running and jumping. *Acta Physiol. Scand.* **174**, 17-30. doi:10.1046/j.1365-201x.2002.00917.x

Hug, F., Lacourpaille, L., Maisetti, O. and Nordez, A. (2013). Slack length of gastrocnemius medialis and Achilles tendon occurs at different ankle angles. *J. Biomech.* **46**, 2534-2538. doi:10.1016/j.jbiomech.2013.07.015

Kim, M. W., Kim, J. H., Yang, Y. J. and Ko, Y. J. (2005). Anatomic localization of motor points in gastrocnemius and soleus muscles. *Am. J. Phys. Med. Rehabil.* **84**, 680-683. doi:10.1097/01.phm.0000176341.85398.a9

Kinugasa, R., Kawakami, Y. and Fukunaga, T. (2005). Muscle activation and its distribution within human triceps surae muscles. *J. Appl. Physiol.* **99**, 1149-1156. doi:10.1152/japplphysiol.01160.2004

Landin, D., Thompson, M. and Reid, M. (2015). Knee and ankle joint angles influence the plantarflexion torque of the gastrocnemius. *J. Clin. Med. Res.* **7**, 602-606. doi:10.14740/jocmr2107w

Lenhart, R. L., Francis, C. A., Lenz, A. L. and Thelen, D. G. (2014). Empirical evaluation of gastrocnemius and soleus function during walking. *J. Biomech.* **47**, 2969-2974. doi:10.1016/j.jbiomech.2014.07.007

Liu, C. L., Zhou, J. P., Sun, P. T., Chen, B. Z., Zhang, J., Tang, C. Z. and Zhang, Z. J. (2020). Influence of different knee and ankle ranges of motion on the elasticity of triceps surae muscles, Achilles tendon, and plantar fascia. *Sci. Rep.* **10**, 6643. doi:10.1038/s41598-020-63730-0

Maas, H. and Finni, T. (2018). Mechanical coupling between muscle-tendon units reduces peak stresses. *Exerc. Sport Sci. Rev.* **46**, 26-33. doi:10.1249/JES.0000000000000132

Maas, H., Noort, W., Baan, G. C. and Finni, T. (2020). Non-uniformity of displacement and strain within the Achilles tendon is affected by joint angle configuration and differential muscle loading. *J. Biomech.* **101**, 109634. doi:10.1016/j.jbiomech.2020.109634

Merletti, R., Knaflitz, M. and Deluca, C. J. (1992). Electrically evoked myoelectric signals. *Crit. Rev. Biomed. Eng.* **19**, 293-340.

Miller, M. S., Callahan, D. M. and Toth, M. J. (2014). Skeletal muscle myofilament adaptations to aging, disease, and disuse and their effects on whole muscle performance in older adult humans. *Front. Physiol.* **5**, 369. doi:10.3389/fphys.2014.00369

Miyoshi, T., Nakazawa, K., Tanizaki, M., Sato, T. and Akai, M. (2006). Altered activation pattern in synergistic ankle plantarflexor muscles in a reduced-gravity environment. *Gait Posture* **24**, 94-99. doi:10.1016/j.gaitpost.2005.07.010

Narici, M. V., Maffulli, N. and Maganaris, C. N. (2008). Ageing of human muscles and tendons. *Disabil. Rehabil.* **30**, 1548-1554. doi:10.1080/09638280701831058

Slane, L. C. and Thelen, D. G. (2014). Non-uniform displacements within the Achilles tendon observed during passive and eccentric loading. *J. Biomech.* **47**, 2831-2835. doi:10.1016/j.jbiomech.2014.07.032

Stewart, C., Postans, N., Schwartz, M. H., Rozumalski, A. and Roberts, A. (2007). An exploration of the function of the triceps surae during normal gait using functional electrical stimulation. *Gait Posture* **26**, 482-488. doi:10.1016/j.gaitpost.2006.12.001

Szaro, P., Witkowski, G., Smigielski, R., Krajewski, P. and Ciszek, B. (2009). Fascicles of the adult human Achilles tendon – an anatomical study. *Ann. Anat.* **191**, 586-593. doi:10.1016/j.aanat.2009.07.006

Thelen, D. G., Lenz, A. L., Francis, C., Lenhart, R. L. and Hernandez, A. (2013). Empirical assessment of dynamic hamstring function during human walking. *J. Biomech.* **46**, 1255-1261. doi:10.1016/j.jbiomech.2013.02.019

Thorpe, C. T., Godinho, M. S. C., Riley, G. P., Birch, H. L., Clegg, P. D. and Screen, H. R. C. (2015). The interfascicular matrix enables fascicle sliding and recovery in tendon, and behaves more elastically in energy storing tendons. *J. Mech. Behav. Biomed. Mater.* **52**, 85-94. doi:10.1016/j.jmbbm.2015.04.009

Thorpe, C. T., Riley, G. P., Birch, H. L., Clegg, P. D. and Screen, H. R. C. (2016). Fascicles and the interfascicular matrix show adaptation for fatigue resistance in energy storing tendons. *Acta Biomater.* **42**, 308-315. doi:10.1016/j.actbio.2016.06.012

Tian, M., Herbert, R. D., Hoang, P., Gandevia, S. C. and Bilston, L. E. (2012). Myofascial force transmission between the human soleus and gastrocnemius muscles during passive knee motion. *J. Appl. Physiol.* **113**, 517-523. doi:10.1152/japplphysiol.00111.2012

Tijs, C., Van Dieen, J. H., Baan, G. C. and Maas, H. (2016). Synergistic Co-activation increases the extent of mechanical interaction between rat ankle plantar-flexors. *Front. Physiol.* **7**, 414. doi:10.3389/fphys.2016.00414

Van Gils, C. C., Steed, R. H. and Page, J. C. (1996). Torsion of the human Achilles tendon. *J. Foot Ankle Surg.* **35**, 41-48. doi:10.1016/S1067-2516(96)80011-1

Wolfram, S., Hodson-Tole, E. F., Morse, C. I., Winwood, K. L. and Mcewan, I. M. (2020). Elongation differences between the sub-tendons of gastrocnemius medialis and lateralis during plantarflexion in different frontal plane position of the foot. *Gait Posture* **75**, 149-154. doi:10.1016/j.gaitpost.2019.10.020